PHYSICAL REVIEW B **77**, 121303(R) (2008)

Precession of localized spins in an inhomogeneous magnetic fringe field

S. Halm,* P. E. Hohage, J. Nannen, and G. Bacher
Werkstoffe der Elektrotechnik, Universität Duisburg-Essen, Bismarckstraße 81, D-47057 Duisburg, Germany

J. Puls and F. Henneberger
Institut für Physik, Humboldt-Universität Berlin, Newtonstraße 15, D-12489 Berlin, Germany

(Received 14 January 2008; published 24 March 2008)

The influence of inhomogeneity of a magnetic fringe field on the coherent spin dynamics of localized manganese impurities in a diluted magnetic semiconductor quantum well is studied by time-resolved Kerr rotation. It is shown that the spatially varying fringe field leads to a temporally varying ensemble precession frequency and a reduced ensemble spin dephasing time T_2^*, which can be modeled by taking into account the local fringe field distribution.

DOI: 10.1103/PhysRevB.77.121303 PACS number(s): 78.47.−p, 85.75.−d, 75.75.+a, 78.20.Ls

One of the central aims of spintronics is to gain control over the spin degree of freedom of charge carriers in semiconductors (SCs).[1] Since the spin is accompanied by a magnetic moment, it can be manipulated by a magnetic field, either an internal field resulting from an electric field[2–4] or strain[5] and spin-orbit coupling or an external field applied, e.g., by ferromagnets (FMs). In general, local spin control is achieved by restricting the field to a confined volume, e.g., with the help of nanostructured electrical or magnetic gates, leading to an inhomogeneous field distribution in the SC. The inhomogeneity can have both desired and detrimental effects: Taking nanoscale FMs as an example, fringe field gradients are proposed to be employed for coherent single electron spin control in a quantum dot[6] and as a spin selective energy trap for carriers in FM-diluted magnetic semiconductor (DMS) hybrid structures.[7] It has been shown by micro-magneto-photoluminescence spectroscopy that a FM fringe field can be used to define and manipulate a spatially varying spin polarization in an underlying DMS quantum well (QW).[8,9] Utilizing the fringe field inhomogeneity, the precession frequency of conduction band carriers in an InGaAs/GaAs quantum well (QW) was modulated on ns time scale by applying voltage pulses to the FMs and dragging the carriers laterally.[10] However, the spin dephasing time of a carrier spin ensemble in presence of an inhomogeneous fringe field is found to be strongly reduced.[11]

Here, we demonstrate how the inhomogeneity of a fringe field originating from nanoscale FMs affects the coherent dynamics of a spin ensemble in an adjacent SC. Since spins of itinerant carriers such as electrons or holes average over at least some part of the inhomogeneity, we use a localized spin system, namely, paramagnetic Mn moments in a (Zn,Cd,Mn)Se/ZnSe QW, as local probes for the inhomogeneous fringe field. A coherent oscillation of the Mn spins is induced via the coherent spin transfer from optically generated, spin polarized carriers.[12] In addition to its localized nature, the Mn spin system is especially suited for our purposes because its g factor is almost independent of the host crystal's band structure, therefore excluding effects of strain, laser excitation energy, temperature, etc., on the precession frequency. We show that the inhomogeneity of the fringe field leads to an ensemble response that qualitatively differs from a simple damped sinusoidal oscillation. The precession frequency of the ensemble varies with the pump-probe delay time, and the ensemble spin dephasing time T_2^* is strongly reduced as compared to a reference area without FMs.

The DMS QW, consisting of 18 monolayers of (Zn,Cd,Mn)Se with a Mn concentration of $x_{\mathrm{Mn}}=0.08$, was grown by molecular beam epitaxy on a (001) GaAs substrate and a 1 μm thick ZnSe buffer. The QW was capped by 25 nm of ZnSe. FM Co wires with varying width and period, a length of 150 μm and a height of 55 nm were processed into arrays of (150×150) μm^2 onto the SC by electron beam lithography, sputtering and lift-off techniques. A cap layer of 5 nm Cr was thermally evaporated onto the FMs to reduce oxidation.

Time-resolved Kerr rotation technique (TRKR) is employed to measure the coherent spin dynamics of localized Mn impurities in the DMS QW. The sample is mounted in a liquid helium flow cryostat and cooled to a temperature of $T=2.3$ K. When an external magnetic field $\boldsymbol{B}_{\mathrm{ext}}=B_{\mathrm{ext}}\cdot\hat{\boldsymbol{x}}$ is applied along the sample surface (Voigt geometry) and perpendicular to the long axis of the FM wires, a magnetic fringe field $\boldsymbol{B}_{\mathrm{fr}}=B_{\mathrm{fr},x}\cdot\hat{\boldsymbol{x}}+B_{\mathrm{fr},z}\cdot\hat{\boldsymbol{z}}$ is created by the FMs (with $\hat{\boldsymbol{x}}$ and $\hat{\boldsymbol{z}}$ being the unit vectors along the directions of $\boldsymbol{B}_{\mathrm{ext}}$ and the sample plane normal, respectively). The Mn spins will then align along the direction of the total magnetic field $\boldsymbol{B}_{\mathrm{tot}}=\boldsymbol{B}_{\mathrm{ext}}+\boldsymbol{B}_{\mathrm{fr}}$. A circularly polarized pump pulse of a frequency doubled, mode-locked titanium:sapphire laser ($\lambda_{\mathrm{pump}}=459.7$ nm, pulse width $\sim$2 ps, repetition rate 76 MHz) resonantly creates electron-heavy-hole pairs in the DMS, whose spins are oriented perpendicular to the QW plane (along $\hat{\boldsymbol{z}}$). Via the hole exchange field the Mn spins are tipped away from their initial orientation and start to precess about $\boldsymbol{B}_{\mathrm{tot}}$.[12–14] The helicity of the pump pulse is modulated at a frequency of 50 kHz by a photoelastic modulator for lock-in detection technique. The $\hat{\boldsymbol{z}}$ component of the Mn magnetization (polar TRKR configuration) is monitored via the Kerr rotation angle $\theta(\Delta t)$ of a linearly polarized probe pulse ($\lambda_{\mathrm{probe}}=\lambda_{\mathrm{pump}}$), which is delayed by the time Δt with respect to the pump pulse. The pump and probe laser beams were focused to a spot diameter of about 20 μm and had a power of 4.6 and 1.3 mW, respectively.

Figure 1 shows the TRKR signal measured on an unstructured reference area of the DMS and on an area covered by

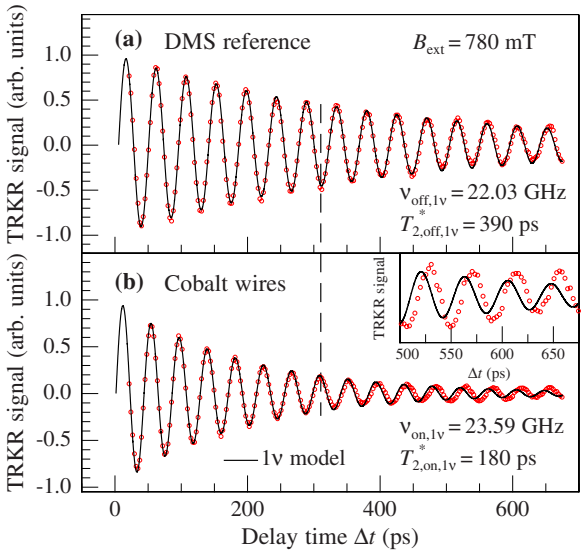

FIG. 1. (Color online) TRKR signal (a) on DMS reference area and (b) on Co wires at B_{ext}=780 mT (inset: enlarged view for 500 ps$\leq\Delta t\leq$675 ps). Solid lines show single frequency (1ν) damped sinusoidal fits to the data.

Co wires (wire width=480 nm, periodicity=1100 nm) in an external field of B_{ext}=780 mT. The data are fitted in the range of 0 ps$\leq\Delta t\leq$300 ps by a damped sinusoidal oscillation [1ν model] of the form

$$\theta(\Delta t) = \theta_0 \exp(-\Delta t/T_2^*)\sin(2\pi\nu\Delta t + \varphi), \qquad (1)$$

where T_2^* is the dephasing time of the Mn spin ensemble, φ is a small phase resulting from the coherent spin transfer from the carrier spins to the Mn spins,[14] and $\nu = g_{Mn}\mu_B\langle B_{tot}\rangle/h$ is the precession frequency. The latter is given by the Mn g factor g_{Mn}=2.01,[13] the Bohr magneton μ_B, Planck's constant h, and the mean total magnetic field $\langle B_{tot}\rangle$, which is averaged over the sample area illuminated by the laser spot. Note that the opaque Co structures act as a shadow mask so that the TRKR signal mainly probes the impact of the fringe field on the DMS in between the structures. The fringe field $\boldsymbol{B}_{fr}$ leads to an enhancement of $\langle B_{tot}\rangle$ which is evidenced by a considerable increase in the observed Mn precession frequency in presence of the Co wires [see dashed line in Fig. 1]. We obtain a frequency shift of $\Delta\nu = \nu_{on,1\nu} - \nu_{off,1\nu}$=1.56 GHz at B_{ext}=780 mT, which is equivalent to a difference between mean total and external magnetic field of $\langle B_{tot}\rangle - B_{ext}$=+55 mT. The dephasing time of the Mn spin ensemble is reduced by the inhomogeneous fringe field from $T^*_{2,off,1\nu}$=390 ps (reference) to $T^*_{2,on,1\nu}$=180 ps (on Co wires).

Fitting the data obtained on the Co wires by formula (1) reveals an interesting feature: the observed precession frequency of the Mn spin ensemble is not constant, but changes with the pump-probe delay time Δt leading to a pronounced phase shift between the data and the fit for larger Δt [see inset in Fig. 1(b)]. The reason for this behavior lies in the field inhomogeneity probed by the localized Mn spins. Since each spin experiences a slightly different but temporally

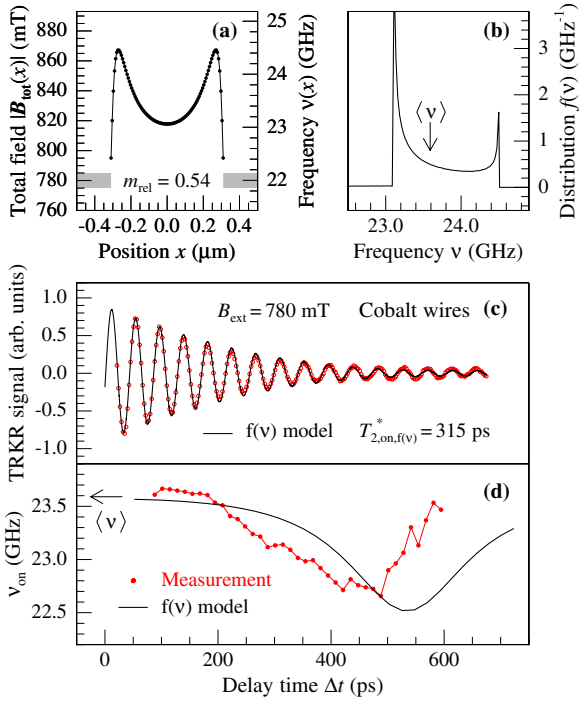

FIG. 2. (Color online) $f(\nu)$ model describing the TRKR signal on the Co FMs. (a) Calculated total magnetic field $B_{tot}(x)$ and precession frequency $\nu(x)$ between two homogeneously magnetized Co wires (indicated by the gray bars) with m_{rel}=0.54 at B_{ext}=780 mT. (b) Frequency distribution $f(\nu)$ resulting from $B_{tot}(x)$. (c) TRKR signal and $f(\nu)$ model at B_{ext}=780 mT. (d) Ensemble precession frequency ν_{on} as a function of delay time Δt compared to the $f(\nu)$ model.

fixed total magnetic field $\boldsymbol{B}_{tot}$, which depends on its spatial position between the Co wires, the ensemble response will be a superposition of individual precessions at different frequencies ν about different axes. Depending on the type of frequency distribution $f(\nu)$, this can lead as in our case to a nonconstant ensemble frequency.

To model the data, we assume a set of uncoupled, localized individual Mn spins oscillating at frequencies $\nu(x)$ about the total magnetic field $\boldsymbol{B}_{tot}(x)$ at positions x [$f(\nu)$ model]. For the sake of simplicity and to minimize the number of free parameters, we assume a homogeneous magnetization of the Co wires along $\hat{\boldsymbol{x}}$ and a uniform illumination by the laser. The total magnetic field $B_{tot}(x) = |\boldsymbol{B}_{fr}(x) + \boldsymbol{B}_{ext}|$ between two adjacent wires at the position of the QW and the resulting precession frequencies $\nu(x)$ are shown for B_{ext}=780 mT in Fig. 2(a) [for details of the calculation of $\boldsymbol{B}_{fr}(x)$ see Ref. 15]. Between the wires it is $B_{fr,x}(x) > 0$ and thus $B_{tot}(x) > B_{ext}$, yielding an increase of the Mn precession frequency. The response of the Mn spin ensemble is described by

$$\theta(\Delta t) = \theta_0 \exp(-\Delta t/T^*_{2,on,f(\nu)}) \sum_i \sin[2\pi\nu(x_i)\Delta t + \varphi]\cos\alpha_i, \qquad (2a)$$

where x_i are the lateral positions of each Mn spin, $T^*_{2,on,f(\nu)}$ is their decoherence time, which in our model is supposed to be identical for each Mn spin, and α_i are the angles between

$\boldsymbol{B}_{\mathrm{tot}}(x_i)$ and $\boldsymbol{B}_{\mathrm{ext}}$ at positions x_i. The factor $\cos\alpha_i$ in Eq. (2a) arises from the projection of the spin precession about $\boldsymbol{B}_{\mathrm{tot}}(x_i)$ onto the $\hat{z}$ direction, that is probed by our polar TRKR setup. In most cases, however, α_i is small because $B_{\mathrm{fr},z} \ll (B_{\mathrm{ext}}+B_{\mathrm{fr},x})$, so that $\cos\alpha_i=1$ can be assumed in a linear approximation. Please note furthermore, that $T^*_{2,\mathrm{on},f(\nu)}$ is not identical to the spin coherence time T_2 of an isolated Mn spin, because $T^*_{2,\mathrm{on},f(\nu)}$ still includes all other possible ensemble dephasing mechanisms in addition to the fringe field inhomogeneity. Since the distance between neighboring Mn spins is short compared to the Co wire separation, the sum in Eq. (2a) can be replaced by an integral. A quasicontinuous frequency distribution $f(\nu)=c dx/d\nu$ can be defined [see Fig. 2(b)], with c being a constant given by the normalization condition $\int_{-\infty}^{\infty} f(\nu)d\nu=1$. Equation (2a) can then be rewritten as

$$\theta(\Delta t) = \theta_0 \exp(-\Delta t/T^*_{2,\mathrm{on},f(\nu)}) \int_{-\infty}^{\infty} f(\nu)\sin(2\pi\nu\Delta t+\varphi)d\nu,$$

$$\overset{\varphi=0}{\theta(\Delta t)} = \sqrt{2\pi}\theta_0 \exp(-\Delta t/T^*_{2,\mathrm{on},f(\nu)})\ \mathrm{Im}\{\mathrm{Fourier}[f(\nu)]\}, \tag{2b}$$

where $\mathrm{Im}\{\mathrm{Fourier}[f(\nu)]\}$ is the imaginary part of the Fourier transform of $f(\nu)$. The two peaks occurring in $f(\nu)$ result from the regions in $\nu(x)$ where $d\nu/dx=0$ (i.e., in the center between two adjacent wires, and close to their edges). The mean frequency $\langle\nu\rangle$ indicated by the arrow is given by $\langle\nu\rangle = \int_{-\infty}^{\infty} f(\nu)\nu d\nu$. Note that the exponential damping of each sinusoidal was not included in our definition of $f(\nu)$.

As Fig. 2(c) shows, the $f(\nu)$ model gives a rather good description of the data. Only two free parameters have been used: the relative magnetization of the Co wires $m_{\mathrm{rel}} = M/M_{\mathrm{sat,Co}}=0.54$ (with $M_{\mathrm{sat,Co}}=1820$ mT/μ_0 (Ref. 16) being the saturation magnetization of Co at 0 K and μ_0 the vacuum permeability) and the spin coherence time $T^*_{2,\mathrm{on},f(\nu)} = 315$ ps. The value of m_{rel} was chosen such that the theoretical mean frequency $\langle\nu\rangle$ coincides with the experimentally determined value of $\nu_{\mathrm{on},1\nu}=23.59$ GHz from Fig. 1. $T^*_{2,\mathrm{on},f(\nu)}$ is close to the reference ensemble value without fringe field $T^*_{2,\mathrm{off},1\nu}$ and significantly larger than the value obtained for the spin ensemble in presence of the Co wires $T^*_{2,\mathrm{on},1\nu}$. A detailed discussion of both parameters and their dependence on the external magnetic field follows in Fig. 3.

In Fig. 2(d) we evaluated the temporal variation of the ensemble precession frequency in presence of the FMs $\nu_{\mathrm{on}}(\Delta t)$ by fitting damped sinusoidal oscillations to the TRKR data in the range of $[\Delta t-65\ \mathrm{ps},\ \Delta t+65\ \mathrm{ps}]$ and extracting ν_{on} as a function of delay time Δt (red curve). For comparison, the black solid line shows the prediction by the $f(\nu)$ model. Both curves show a qualitatively similar behavior, i.e., a reduction of ν_{on} by $\sim$1 GHz during the first $\sim$500 ps followed by an increase to (almost) the initial frequency. A quantitatively accurate description cannot be expected from our simple model because both the exact local fringe field distribution resulting from the nonperfect rectangular shape of the magnets as well as the laterally inhomogeneous laser illumination profile between the Co wires (due to near-field diffraction) are not included. Two points are worth emphasizing: First, the modeled ensemble frequency ν_{on} coincides for small Δt with the mean frequency $\langle\nu\rangle$, which is true for any given $f(\nu)$. Second, while all nondiscrete frequency distributions lead to a reduced ensemble decoherence time, only those which are asymmetric with respect to their mean value $\langle\nu\rangle$ will show a temporally varying precession frequency. This is the case for the $f(\nu)$ resulting from a fringe field [see Fig. 2(b)], but not, e.g., for a Lorentzian or Gaussian frequency distribution.

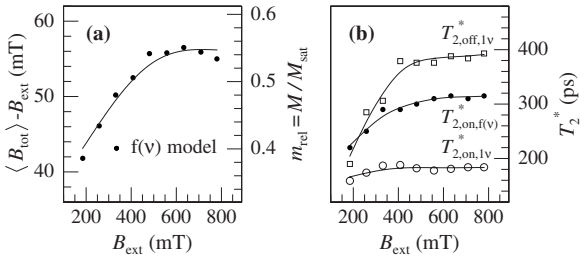

FIG. 3. (a) Magnetic field dependence of mean fringe field contribution $\langle B_{\mathrm{tot}}\rangle - B_{\mathrm{ext}} \approx \langle B_{\mathrm{fr},x}(x)\rangle$ (left axis) and relative magnetization m_{rel} (right axis) using the $f(\nu)$ model. (b) Mn spin ensemble dephasing times with ($T^*_{2,\mathrm{on},1\nu}$) and without ($T^*_{2,\mathrm{off},1\nu}$) fringe field as well as coherence time of each Mn spin ($T^*_{2,\mathrm{on},f(\nu)}$) within the $f(\nu)$ model. All solid lines are guides to the eye.

Figure 3 summarizes the results for varying external magnetic field B_{ext}. Figure 3(a) shows the mean value of $\langle B_{\mathrm{tot}}\rangle - B_{\mathrm{ext}}$ (left axis) and the relative magnetization m_{rel} (right axis) of the Co wires according to the $f(\nu)$ model. Since, except for the very FM edges, the precession axes of the Mn spins lie close to the sample plane (i.e., the α_i are small, typically $<1°$), the following approximation can be made

$\langle B_{\mathrm{fr},x}\rangle = \langle B_{\mathrm{tot}}\cos\alpha\rangle - B_{\mathrm{ext}} \approx \langle B_{\mathrm{tot}}\rangle - B_{\mathrm{ext}}$, which demonstrates that mainly the $\hat{x}$ component of the fringe field is probed in the experiment. It can be seen that $\langle B_{\mathrm{tot}}\rangle - B_{\mathrm{ext}}$ and m_{rel} increase up to $B_{\mathrm{ext}}\approx 0.5$ T and then saturate, a behavior that has similarly been observed by magneto-optical Kerr effect (MOKE) on 80-nm-thick Fe wires with a width of 500 nm and a periodicity of 1 μm.[11] The fact that the model parameter m_{rel} saturates at a value much lower than 1 indicates that the FMs do not consist of pure Co but might be partially oxidized, an assumption that is supported by energy-dispersive x-ray spectroscopy data performed on our FM structures. We can exclude in our sample that negative fringe field components from the areas shadowed by the FMs play a major role in the observed $\langle B_{\mathrm{tot}}\rangle - B_{\mathrm{ext}}$ (and thus in m_{rel}), because this would lead to a large, qualitative difference between the modeled and the observed behavior of $\nu_{\mathrm{on}}(\Delta t)$ in Fig. 2(c).

Figure 3(b) depicts the dephasing times of the Mn spin ensemble in presence of the Co wires ($T^*_{2,\mathrm{on},1\nu}$) and on an unstructured reference area ($T^*_{2,\mathrm{off},1\nu}$) as extracted from single frequency, damped sinusoidal fits, as well as the $f(\nu)$ model parameter $T^*_{2,\mathrm{on},f(\nu)}$. First, it can be seen that $T^*_{2,\mathrm{off},1\nu}$ in the reference increases with external field, which has been observed before.[13] $T^*_{2,\mathrm{on},1\nu}$ on the Co structures does not increase in the same way as $T^*_{2,\mathrm{off},1\nu}$, suggesting that the locally inhomogeneous fringe field $\boldsymbol{B}_{\mathrm{fr}}$, which increases with B_{ext},

efficiently reduces the experimentally observed ensemble spin dephasing time. This assumption is confirmed by the values of $T^*_{2,\mathrm{on},f(\nu)}$ [the coherence time of each Mn spin within the $f(\nu)$ model], which follow the reference measurement closely. Hence, the major part of the additional ensemble decoherence in presence of a fringe field can be assigned to its inhomogeneity, which leads to varying individual precession frequencies and directions of the Mn spins. The reason why $T^*_{2,\mathrm{off},1\nu}$ and $T^*_{2,\mathrm{on},f(\nu)}$ do not fully coincide is not clarified so far but might be due to the fact that adjacent Mn spins are not completey uncoupled as assumed in the model but experience a short-range, antiferromagnetic coupling.[17] The coupling may enhance the dephasing of neighboring spins oscillating at slightly different frequencies about slightly different axes.

In summary, we have shown that the inhomogeneity of a local magnetic fringe field originating from nanostructured FMs leads to a temporal variation of the ensemble precession frequency and an additional dephasing of a localized spin ensemble. We would like to note that this behavior is not restricted to the special case of magnetic fringe fields but has a more general importance. Any inhomogeneity, either in magnetic field, in electric field with spin-orbit interaction, or in g factor, which results in an asymmetric frequency distribution, will have the same consequences for any localized spin ensemble.

The authors gratefully acknowledge the sample preparation by F. Seifert and the financial support of the Deutsche Forschungsgemeinschaft within the priority program SPP 1133 and by the Sonderforschungsbereich 491.

*simon.halm@uni-due.de

[1] S. A. Wolf *et al.*, Science **294**, 1488 (2001).
[2] S. Datta and B. Das, Appl. Phys. Lett. **56**, 665 (1990).
[3] E. I. Rashba and Al. L. Efros, Phys. Rev. Lett. **91**, 126405 (2003).
[4] L. Meier, G. Salis, I. Shorubalko, E. Gini, S. Schön, and K. Ensslin, Nat. Phys. **3**, 650 (2007)
[5] Y. K. Kato, R. C. Myers, A. C. Gossard, and D. D. Awschalom, Nature (London) **427**, 50 (2004).
[6] Y. Tokura, W. G. van der Wiel, T. Obata, and S. Tarucha, Phys. Rev. Lett. **96**, 047202 (2006).
[7] P. Redliński, T. Wojtowicz, T. G. Rappoport, A. Libál, J. K. Furdyna, and B. Jankó, Phys. Rev. B **72**, 085209 (2005).
[8] A. Murayama and M. Sakuma, Appl. Phys. Lett. **88**, 122504 (2006).
[9] S. Halm, G. Bacher, E. Schuster, W. Keune, M. Sperk, J. Puls, and F. Henneberger, Appl. Phys. Lett. **90**, 051916 (2007).
[10] L. Meier, G. Salis, C. Ellenberger, E. Gini, and K. Ensslin, Phys. Rev. B **74**, 245318 (2006).
[11] L. Meier, G. Salis, C. Ellenberger, K. Ensslin, and E. Gini, Appl. Phys. Lett. **88**, 172501 (2006).
[12] S. A. Crooker, J. J. Baumberg, F. Flack, N. Samarth, and D. D. Awschalom, Phys. Rev. Lett. **77**, 2814 (1996).
[13] S. A. Crooker, D. D. Awschalom, J. J. Baumberg, F. Flack, and N. Samarth, Phys. Rev. B **56**, 7574 (1997).
[14] R. Akimoto, K. Ando, F. Sasaki, S. Kobayashi, and T. Tani, Phys. Rev. B **57**, 7208 (1998).
[15] S. Halm, P. E. Hohage, E. Neshataeva, F. Seifert, T. Kümmell, E. Schuster, W. Keune, M. Sperl, Y.-H. Fan, J. Puls, F. Henneberger, and G. Bacher, Phys. Status Solidi A **204**, 191 (2007).
[16] F. Keffer, *Handbuch der Physik*, edited by S. Flügge (Springer-Verlag, Berlin, Germany, 1966), Vol. 18, Pt. 2, p. 4.
[17] *Diluted Magnetic Semiconductors*, edited by J. K. Furdyna and J. Kossut (Academic, New York, 1988).